

Asteroid project summary

Jack Dinsmore, Julien de Wit

November 11, 2021

1 Introduction

2 Asteroid Model

In an effort to make a general asteroid model, we will consider the entire effect of the tidal torque applied to an asteroid from a planet, rather than solving for the first order perturbation. To better understand the effect, we will not model perturbing effects from other bodies such as the Sun or other planets. However, nearby bodies, such as moons or rings, are considered in a later section. We will also model the asteroid as a rigid body, whose density distribution is fixed throughout the flyby.

Most asteroids are observed to have attained their minimum energy rotation state, so we will also assume that the asteroid's initial state aligns its rotational velocity parallel to the principal axis with maximal moment of inertia.

2.1 Coordinates

We will make use of two frames of reference to model this system. One is the “inertial frame,” with axes denoted by $\hat{\mathbf{X}}, \hat{\mathbf{Y}}, \hat{\mathbf{Z}}$. As the name suggests, these axes are inertial, with $\hat{\mathbf{X}}$ pointing to the asteroid pericenter and $\hat{\mathbf{Z}}$ pointing parallel to the orbit angular momentum. The origin of this frame is set to the center of mass of the central body. We will assume that the mass distribution of the central body is known in this inertial frame.

Our second frame is the “body-fixed” frame, denoted by $\hat{\mathbf{x}}, \hat{\mathbf{y}}, \hat{\mathbf{z}}$. This frame is fixed with respect to the body's principle axes and rotates with the body, with its origin at the body's center of mass. We will solve for the asteroid's mass distribution with reference to the body-fixed frame. For definiteness, we define $\hat{\mathbf{z}}$ to be the principal axis with maximal MOI, and $\hat{\mathbf{x}}$ to have minimal MOI.

We define a rotation matrix M such that $M\mathbf{r} = \mathbf{R}$, where \mathbf{r} is in the body-fixed frame and \mathbf{R} is in the inertial frame. We write this matrix in terms of the $z - y - z$ Euler angles, named α, β , and γ , defined in figure 1. These Euler angles, together with the position and momentum of the asteroid, are our dynamical variables.

2.2 Potential energy

We start by expressing the gravitational potential energy of the system in its most general form:

$$V = -G \int_{\mathcal{A}} d^3r' \rho_m(\mathbf{r}') \int_{\mathcal{P}} d^3r \rho_M(\mathbf{r}) \frac{1}{|\mathbf{r} - \mathbf{r}'|}. \quad (1)$$

This integral is computed in the inertial frame. Here, $\boldsymbol{\omega}$ is the rotational velocity of the asteroid and I is the inertia tensor, both in the body fixed frame. We also use the asteroid density ρ_m and

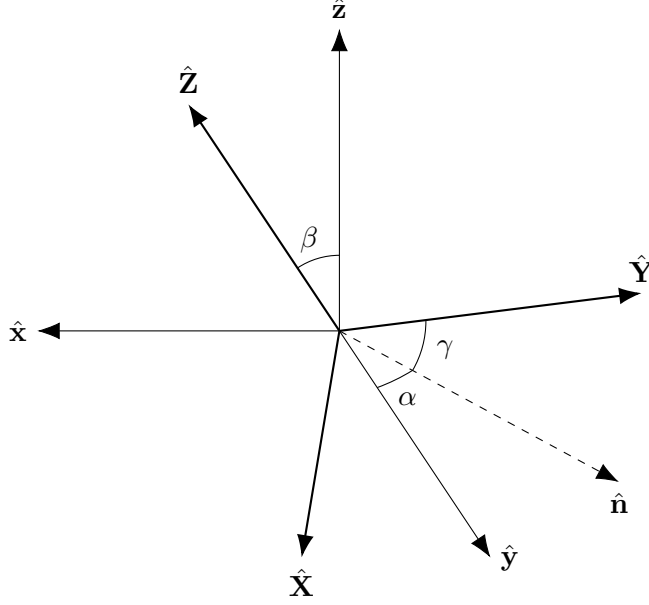


Figure 1: $z - y - z$ Euler angles used in this work to express the orientation of the asteroid. Orientation is expressed as a rotation from the body-fixed axes to the inertial axes.

the central body density ρ_M . The symbol \mathcal{A} denotes the volume of the asteroid and \mathcal{P} denotes the volume of the central body. To reduce equation 1, we define the unnormalized spherical harmonics $Y_{\ell m}(\theta, \phi) = P_{\ell m}(\cos \theta)e^{im\phi}$, where $P_{\ell m}$ are the associated Legendre Polynomials without the Condon-Shortley phase. The regular and irregular spherical harmonics are then defined as

$$S_{\ell m}(\mathbf{r}) = (-1)^m (\ell - m)! \frac{Y_{\ell m}(\hat{\mathbf{r}})}{r^{\ell+1}} \quad R_{\ell m}(\mathbf{r}) = (-1)^m \frac{r^\ell}{(\ell + m)!} Y_{\ell m}(\hat{\mathbf{r}}). \quad (2)$$

Assume that we can construct a sphere, centered at the center of mass of the central body, so that $\rho_M = 0$ outside the sphere and $\rho_m = 0$ inside the sphere. Then $r' > r$ in equation 1, and Ref. [1] gives the identity

$$\frac{1}{|\mathbf{r} - \mathbf{r}'|} = \sum_{\ell, m} R_{\ell m}(\mathbf{r}) S_{\ell m}^*(\mathbf{r}'), \quad (3)$$

where the sum is shorthand for $\sum_{\ell, m} = \sum_{\ell=0}^{\infty} \sum_{m=-\ell}^{\ell}$.

Suppose the vector \mathbf{D} points from the center of mass of the central body to the center of mass of the asteroid. Then we may write $\mathbf{r}' = \mathbf{D} + \mathbf{u}$, and Ref. [1] gives

$$S_{\ell m}(\mathbf{r}') = \sum_{\ell', m'} (-1)^{\ell'} R_{\ell' m'}^*(\mathbf{u}) S_{\ell+\ell', m+m'}(\mathbf{D}). \quad (4)$$

Let us define complex, unitless constants

$$J_{\ell m} = \int_{\mathcal{P}} d^3 r \rho_M(\mathbf{r}) \frac{R_{\ell m}(\mathbf{r})}{\mu_M a_M^\ell} \quad K_{\ell m} = \int_{\mathcal{P}} d^3 r \rho_m(\mathbf{r}) \frac{R_{\ell m}(\mathbf{r})}{\mu_m a_m^\ell} \quad (5)$$

where the integrals are taken in the inertial and the body-fixed frames respectively. The symmetry relations of $R_{\ell m}$ guarantee $J_{\ell m} = (-1)^m J_{\ell, -m}$ and similarly for $K_{\ell m}$. We have chosen μ_M, μ_m to be

the masses of the central body and asteroid respectively, and a_M and a_m to be scale lengths of both bodies (defined more precisely later). Then, by rotating $K_{\ell m}$ from the body-fixed axis orientation to the inertial axis orientation, we may use $J_{\ell m}$ and $K_{\ell m}$ to simplify the potential energy. Rotations of the spherical harmonics are given by the Wigner-D matrices, via the formula

$$Y_{\ell m}(M\mathbf{r}) = \sum_{m'=-\ell}^{\ell} \mathcal{D}_{mm'}^{\ell}(M)^* Y_{\ell m'}(\mathbf{r}). \quad (6)$$

The corollary of this formula for the regular solid spherical harmonic is

$$R_{\ell m}(M\mathbf{r}) = \sum_{m'=-\ell}^{\ell} (-1)^{m+m'} \frac{(\ell+m')!}{(\ell+m)!} \mathcal{D}_{mm'}^{\ell}(M)^* R_{\ell m'}(\mathbf{r}) \quad (7)$$

where $\mathcal{D}_{mm'}^{\ell}$ are the Wigner-D matrix elements. In practice, these are computed from the Euler angles corresponding to the rotation M , which we specified in section 2.1 are $z-y-z$ Euler angles. With this choice of axes, the Wigner-D matrix elements are real with matrix elements given by

$$d_{mm'}^{\ell}(\beta) = \sqrt{(\ell+m)!(\ell-m)!(\ell+m')!(\ell-m')!} \sum_{s=s_{\min}}^{s_{\max}} \left[\frac{(-1)^{m-m'+s} \left(\cos \frac{\beta}{2}\right)^{2\ell+m'-m-2s} \left(\sin \frac{\beta}{2}\right)^{m-m'+2s}}{(\ell+m'-s)!(\ell-m-s)!(m-m'+s)!s!} \right] \quad (8)$$

where $s_{\min} = \max(0, m'-m)$ and $s_{\max} = \min(\ell+m', \ell-m)$, and $\mathcal{D}_{mm'}^{\ell}(\alpha, \beta, \gamma) = d_{mm'}^{\ell} e^{-im\alpha} e^{-im'\gamma}$. For neatness, we define the unitless constants

$$C_{\ell\ell'mm'm''}(\alpha, \beta, \gamma, t) = D(t) (-1)^{\ell'+m'+m''} S_{\ell+\ell', m+m'}^* (\mathbf{D}(t)) a_M^{\ell} a_m^{\ell'} \frac{(\ell'+m'')!}{(\ell'+m')!} \mathcal{D}(\mathbf{q})_{m'm''}^{\ell}(M)^* \quad (9)$$

where $\mathbf{D}(t)$ is purely dependent on time because the orbital path of the asteroid is assumed to be Keplerian. Then, combining equations 3 through 8, we get a potential energy of

$$V = -\frac{G\mu_M\mu_m}{D(t)} \sum_{\ell, m} \sum_{\ell', m'} \sum_{m''=-\ell'}^{\ell'} C_{\ell\ell'mm'm''}(\alpha, \beta, \gamma, t) J_{\ell, m} K_{\ell', m''}. \quad (10)$$

2.3 Kinetic energy

The inertia tensor of the asteroid is expressed as a matrix I . Written in terms of spherical harmonics in the body-fixed frame, we have

$$I = \int_{\mathcal{A}} d^3r \rho_m(\mathbf{r}) \begin{pmatrix} y^2 + z^2 & -xy & -xz \\ -xy & x^2 + z^2 & -xz \\ -xz & -yz & x^2 + y^2 \end{pmatrix} \quad (11)$$

$$= \frac{2}{3} \mu_m a_m^2 \begin{pmatrix} K_{20} - 3K_{2,-2} - 3K_{22} + 1 & 3i(K_{22} - K_{2,-2}) & \frac{3}{2}(K_{21} - K_{2,-1}) \\ 3i(K_{22} - K_{2,-2}) & K_{20} + 3K_{2,-2} + 3K_{22} + 1 & -\frac{3}{2}i(K_{21} - K_{2,-1}) \\ \frac{3}{2}(K_{21} - K_{2,-1}) & -\frac{3}{2}i(K_{21} - K_{2,-1}) & -2K_{20} + 1 \end{pmatrix}$$

where we have defined, for neatness,

$$a_m^2 = \frac{1}{\mu_m} \int_{\mathcal{A}} d^3r \rho_m(\mathbf{r}) r^2. \quad (12)$$

With this definition of a_m , and an arbitrary definition of a_M which may be taken to be similar to equation 12 or a more convenient unit such as the central body radius, the parameters $J_{\ell m}$ and $K_{\ell m}$ of equation 5 are completely defined. Note that a_m is similar to the radius of the asteroid; if the asteroid is a sphere of uniform density and radius r , then $a_m = r\sqrt{3/5}$.

Henceforth, we define the body-fixed axis to be coincident with the principal axes of the asteroids, so that the off-diagonal components of I are zero.

To calculate the kinetic energy, we write the angular velocity in the body-fixed frame in terms of the Euler angles:

$$\boldsymbol{\omega}_{xyz} = \begin{pmatrix} 0 & -\sin \alpha & \sin \beta \cos \alpha \\ 0 & \cos \alpha & \sin \beta \sin \alpha \\ 1 & 0 & \cos \beta \end{pmatrix} \begin{pmatrix} \dot{\alpha} \\ \dot{\beta} \\ \dot{\gamma} \end{pmatrix}. \quad (13)$$

The rotational kinetic energy is then

$$K = \frac{1}{2} \boldsymbol{\omega}^T I \boldsymbol{\omega} \quad (14)$$

where $\boldsymbol{\omega}$ and I are both given in the body-fixed frame.

2.4 Hamiltonian and Equations of motion

As a simplifying assumption, we will not model the effect of the central body's non-sphericity on the asteroid orbit. This effect has been studied in much detail and is small. We therefore separate the position dynamical variables from the angular variables and derive the standard equations of motion for asteroid position:

$$\dot{\mathbf{v}} = -\frac{G\mu_M}{r^3} \mathbf{r} \quad \dot{\mathbf{r}} = \mathbf{v}. \quad (15)$$

The position variables will no longer be discussed.

The Lagrangian for the rotating part of the system is $L = T - V$, with kinetic and potential energy given by equations 14 and 10 respectively. Defining $\mathbf{q} = (\alpha, \beta, \gamma)^T$, we can write equation 13 as $\boldsymbol{\omega}_{xyz} = A\dot{\mathbf{q}}$, in which case

$$L = \frac{1}{2} \dot{\mathbf{q}}^T A^T I A \dot{\mathbf{q}} - V_0 \sum_{\ell, m} \sum_{\ell', m'} \sum_{m''=-\ell'}^{\ell'} C_{\ell\ell'mm'm''}(\mathbf{q}, t) J_{\ell, m} K_{\ell' m''}. \quad (16)$$

where $V_0 = -G\mu_M\mu_m/D(t)$ is the Newtonian potential energy of point masses μ_M and μ_m . This corresponds to a Hamiltonian of

$$H = \frac{1}{2} \mathbf{p}^T (A^{-1}(\mathbf{q})) I^{-1} (A^{-1}(\mathbf{q}))^T \mathbf{p} + V_0 \sum_{\ell, m} \sum_{\ell', m'} \sum_{m''=-\ell'}^{\ell'} C_{\ell\ell'mm'm''}(\mathbf{q}, t) J_{\ell, m} K_{\ell' m''} \quad (17)$$

with the conjugate momenta defined as

$$\mathbf{p} = A^T I A \dot{\mathbf{q}} = A^T I \boldsymbol{\omega}_{xyz} \quad \boldsymbol{\omega}_{xyz} = A \dot{\mathbf{q}} = I^{-1} (A^{-1})^T \mathbf{p}. \quad (18)$$

The inverse of A is computed as

$$A^{-1} = \frac{1}{\sin \beta} \begin{pmatrix} -\cos \alpha \cos \beta & -\sin \alpha \cos \beta & \sin \beta \\ -\sin \alpha \sin \beta & \cos \alpha \sin \beta & 0 \\ \cos \alpha & \sin \alpha & 0 \end{pmatrix}. \quad (19)$$

The equations of motion of the system are then a system of six first-order ordinary differential equations:

$$\dot{\mathbf{q}} = \nabla_{\mathbf{p}} H \quad \dot{\mathbf{p}} = -\nabla_{\mathbf{q}} H. \quad (20)$$

We compute these derivatives manually:

$$\dot{\mathbf{q}} = A^{-1} I^{-1} (A^{-1})^T \mathbf{p} \quad (21)$$

and

$$\dot{p}_i = \mathbf{p}^T \frac{\partial A^{-1}}{\partial q_i} I^{-1} (A^{-1})^T \mathbf{p} - V_0 \sum_{\ell, m} \sum_{\ell', m'} \sum_{m''=-\ell'}^{\ell'} J_{\ell, m} K_{\ell' m''} \frac{\partial}{\partial q_i} C_{\ell \ell' m m''}(\mathbf{q}, t). \quad (22)$$

Explicitly, the derivatives of A^{-1} are

$$\begin{aligned} \frac{\partial A^{-1}}{\partial \alpha} &= \frac{1}{\sin \beta} \begin{pmatrix} \sin \alpha \cos \beta & -\cos \alpha \cos \beta & 0 \\ -\cos \alpha \sin \beta & -\sin \alpha \sin \beta & 0 \\ -\sin \alpha & \cos \alpha & 0 \end{pmatrix} \\ \frac{\partial A^{-1}}{\partial \beta} &= \frac{1}{\sin^2 \beta} \begin{pmatrix} \cos \alpha & \sin \alpha & 0 \\ 0 & 0 & 0 \\ -\cos \alpha \cos \beta & -\sin \alpha \cos \beta & 0 \end{pmatrix} \quad \frac{\partial A^{-1}}{\partial \gamma} = 0. \end{aligned} \quad (23)$$

The C coefficients depend on \mathbf{q} through the Wigner-D matrices, which obey

$$\nabla_{\mathbf{q}} \mathcal{D}_{mm'}^{\ell}(\mathbf{q}) = \begin{pmatrix} -im\alpha \mathcal{D}_{mm'}^{\ell}(\mathbf{q}) \\ e^{-im\alpha} e^{-im'\gamma} \frac{\partial}{\partial \beta} d_{mm'}^j \\ -im'\gamma \mathcal{D}_{mm'}^{\ell}(\mathbf{q}) \end{pmatrix}. \quad (24)$$

Finally, the derivative of the matrix elements $d_{mm'}^j$ are given by multiplying each term in the sum over s of equation 8 by

$$\frac{1}{2} \left((m - m' + 2s) \cot \frac{\beta}{2} - (2\ell + m' - m - 2s) \tan \frac{\beta}{2} \right),$$

except when $\beta = 0$ or π . In these cases, the derivative is zero except when $\beta = 0$ and $m - m' + 2s = 1$, or $\beta = \pi$ and $2\ell + m' - m - 2s = 1$, in which case the derivative of the trigonometric functions is $1/2$.

The dynamical variables \mathbf{q}, \mathbf{p} can then be integrated numerically to solve for the full dynamics of the system.

2.5 Initial values

To solve for \mathbf{q}, \mathbf{p} as functions of time, we need their values at some point in time. We study their values far from the central body before the flyby, when they are assumed to be in steady state. Here, the spin axis $\boldsymbol{\omega}$ is parallel to the body-fixed unit axis $\hat{\mathbf{z}}$. This fixes β and γ while α is left free, expressing the initial orientation of the asteroid. Specifically, $\cos \beta = \omega_Z/\omega$ and $\tan \gamma = \omega_Y/\omega_X$.

For the initial conjugate momenta, we use equation 18 and the fact that $\boldsymbol{\omega}_{xyz} = \omega \hat{\mathbf{z}}$ at the initial position. Specifically:

$$\mathbf{p}_0 = \frac{2}{3} \mu_m a_m^2 (-2K_{20} + 1) \omega \begin{pmatrix} 1 \\ 0 \\ \cos \beta \end{pmatrix}. \quad (25)$$

2.6 Fit parameters

By requiring that the $\hat{\mathbf{x}}, \hat{\mathbf{y}}, \hat{\mathbf{z}}$ axes coincide with principal axes, we force the diagonal components of I to be zero. Thus, we may require $K_{21} = K_{2,-1} = 0$ and $\Im K_{22} = \Im K_{2,-2} = 0$ with no loss of generality. By requiring that the body-fixed frame be located at the center of mass of the asteroid, we also require $K_{1m} = 0$. Finally, $K_{00} = 1$ follows automatically from the definition. Thus, K_{20} , $\Re K_{22}$, and $K_{\ell>2,m}$ are the only physical parameters of the asteroid density distribution, beyond a_m .

Note from equation 9 that $C_{\ell=\ell'=0} = 0$. Since $J_{\ell=1} = K_{\ell=1} = 0$ as well, the Hamiltonian in equation 17 is proportional to $\mu_m a_m^2$. Factoring out this product results in a Hamiltonian independent of μ_m , meaning that the asteroid dynamics are unaffected by the mass of the asteroid. This is expected, and it means that the density distribution of the asteroid can only be determined up to a scale factor.

Also note that $C_{\ell\ell'mm'm''} \propto a_M^\ell a_m^{\ell'}/D^{\ell+\ell'}$. Usually, $D \gg a_M \gg a_m$, so we expect this fraction to be small. The nonzero term first order in this fraction in the potential energy has $\ell = 0$ and $\ell' = 2$. To first order in the asteroid density distribution, therefore, the system is also independent of a_m . When $K_{\ell'>2}$ terms are included, a_m scales the size of the higher order terms.

We require that the moment of inertia matrix be positive-definite, which bounds our asteroid parameters. Specifically, we have $K_{20} \leq \frac{1}{2}$, and $|K_{22}| \leq (K_{20}+1)/6$. We can also choose without loss of generality to let the maximum moment of inertia align with $\hat{\mathbf{z}}$, so that $1-2K_{20} \geq K_{20}+1+6|K_{22}|$. Finally, we wish to require that the density of the asteroid be everywhere positive. One consequence of this requirement is that the sum of any two distinct moments of inertia cannot be greater than the third, by the integral definition of moment of inertia in equation 11. Three inequalities result from this, but only one is not covered by the above restrictions. Namely, $I_{xx}+I_{yy} \geq I_{zz} \implies K_{20} \geq -1/4$. The intersection of these requirements forces K_{20} and K_{22} to lie in the triangle defined by

$$-\frac{1}{4} \leq K_{20} \leq 0 \quad |K_{22}| \leq -\frac{K_{20}}{2}. \quad (26)$$

We have one additional fit parameter, which is the only initial condition not fixed by the problem setup or observations. Namely, the initial value of the first Euler angle α_0 . Due to the fact that the principal axes $\hat{\mathbf{x}}$ and $\hat{\mathbf{y}}$ are orthogonal, increments of α_0 by $\pi/2$ correspond to flipping the body-fixed axes so that no physical change in the asteroid model occurs. We must therefore limit the range of α_0 to width $\pi/2$. Arbitrarily, we choose $\alpha_0 \in [-\pi/4, \pi/4]$

3 Experiment design

3.1 Simulation design

Given the observed orbit of an asteroid and observational data of its resolved spin over time, we built a simulation that would integrate equations 22 and 21 to generate synthetic data. Inputs to the simulation were (1) the ℓ and ℓ' values at which to truncate the potential energy sum in equation 10, (2) the cadence of observations, (3) the $J_{\ell m}$ parameters and mass and radius of the central body, (4) a guess at the asteroid parameters $K_{\ell m}$, α_0 and a_m , (5) the initial rotational velocity of the asteroid in the inertial frame, and (6) the asteroid's orbital parameters.

The orbital parameters we use to describe the orbit are the hyperbolic excess velocity v_∞ and the pericenter altitude r_p . The orbit orientation is fixed to lie in the $\hat{\mathbf{X}} - \hat{\mathbf{Y}}$ plane, with pericenter lying on $\hat{\mathbf{X}}$. The position of the satellite as a function of time is therefore generated by numerically integrating the Newtonian equation of motion (equation 15) from initial values $\mathbf{r}(t=0) = r_p \hat{\mathbf{X}}$ and $\mathbf{v}(t=0) = \hat{\mathbf{Y}} \sqrt{v_\infty^2 + 2G\mu_M/r_p}$

Once the inputs were specified, the moments of inertia were pre-computed from $K_{\ell m}$, as was the orbital path of the satellite as a function of time. Equations 22 and 21 were then integrated by the fourth order Runge-Kutta method with a time step of *Insert time step*, with a custom implementation of the spherical harmonics and Wigner-D matrices to improve runtime. At fixed time intervals, the rotational velocity in the body-fixed frame ω_{xyz} was computed via equation 13 from the Euler angles and rotated into the global frame to produce synthetic data.

Since the leading order of the equations of motion is *What is it?*, we begin our simulation at $t = -$ *When do we begin the simulation?* and end at $t = +$, where $t = 0$ is the time at periapsis.

3.2 Fitting method

To analyze the degree to which asteroid density distributions can be determined from flyby rotational velocity data, we use the forward model defined in section 3.1 to generate synthetic data, randomize the data according to one of the observational uncertainty model defined in section 3.3, then use the same forward model to fit to the data and recover parameters.

After randomizing the data, we isolate a set of parameters which are likely to provide good fits. To do this, we minimize the χ^2 value of the data given the model using the BFGS algorithm. Our starting points for the minimization are spaced uniformly randomly across the allowed parameter space, which is the set of parameters with the triangle described by equation 26. The other parameter bounds are $\alpha_0 \in [-\pi/4, \pi/4]$, and $|\Re K_{l>2}| \leq 1$, $|\Im K_{l>2}| \leq 1$.

If the minimization is conducted over too many parameter dimensions, convergence can be slow and potentially inaccurate. However, the parameters $K_{\ell m}$ are naturally separated into groups by order of ℓ , since the torque applied by successive increment to ℓ is suppressed by a_m/D . Thus, we fit the $\ell = 2$ and α_0 parameters first, then lock them in place and fit the $\ell = 3$ parameters, etc. The result is a set of points in parameter space which minimize the χ^2 .

We are interested in finding not just the optimal parameters, but the probability distributions of each fit parameter. To do this, we use an Affine Invariant Markov Chain Monte Carlo Ensemble Sampler (MCMC), implemented in the Python package `emcee`, to conduct the fit to data [2]. This fit method requires the parameter space to be populated with “walkers,” indicating the a guess at the true parameters of the system. We center these walkers on the minimizing parameters computed by the minimization of χ^2 , and spread out the walkers such that the number density of walkers is proportional to the likelihood ($\ln \mathcal{L} = -\chi^2$) at each point. This is done explicitly by computing the Hessian Σ of the likelihood at each minimizing point θ_0 and expressing the likelihood locally as a multi-dimensional Gaussian

$$\mathcal{L}(\theta) \propto \exp\left(\frac{1}{2}(\theta - \theta_0)^T \Sigma (\theta - \theta_0)\right). \quad (27)$$

We may change bases into a frame in which the parameters are uncorrelated by multiplying by D^T , which is the matrix of eigenvectors of Σ . Populating the walkers in this uncorrelated space according to Gaussian standard deviations given by the eigenvalues of Σ , we can convert these walkers back to θ -space by multiplying by D .

With the initial walkers distributed, we use the χ^2 value as the log-likelihood to compute the posterior probability distribution of θ given flat priors in the range outlined above for each parameter.

3.3 Uncertainty models

We model uncertainties in experimental data according to several methods, comparing them to determine the dependence of our conclusions on the sensitivity model used. In every case, the

sensitivity model is used both to add randomness to the data set after it is generated, and to weight the χ^2 statistic.

3.3.1 Nominal method

The most detailed uncertainty model we use, and the one we use most often, is called the “nominal method.” It rotates each angular velocity vector by some angle Θ drawn from a normal distribution centered on $\Theta = 0$ with standard deviation σ_θ . The period is assumed to be known to arbitrary precision at each cadence. The direction in which the velocity is rotated is chosen from a uniformly random distribution. σ_θ is a general parameter which can be tweaked to model resolution of the spin axis direction.

Practically, the randomization of the data is done by creating a rotation matrix M that rotates $\hat{\mathbf{Z}}$ to the true rotational velocity vector $\boldsymbol{\omega}$. This same rotation matrix is then used to rotate the random vector $\boldsymbol{\Omega} = \sin \Theta \cos \Phi \hat{\mathbf{X}} + \sin \Theta \sin \Phi \hat{\mathbf{Y}} + \cos \Theta \hat{\mathbf{Z}}$ to the randomized velocity vector. Here, Φ is a uniformly random variable in the range $[0, \pi)$. Specifically, we write this rotation matrix as

$$M = \begin{pmatrix} \cos \phi & -\sin \phi & 0 \\ \sin \phi & \cos \phi & 0 \\ 0 & 0 & 1 \end{pmatrix} \begin{pmatrix} \cos \theta & 0 & \sin \theta \\ 0 & 1 & 0 \\ -\sin \theta & 0 & \cos \theta \end{pmatrix} \quad (28)$$

where θ and ϕ are the spherical coordinates of the original velocity vector $\boldsymbol{\omega}$.

Equation 28 is sufficient to randomize synthetic data, but an analytical expression for the coordinates of $\boldsymbol{\omega}$ is required to define the χ^2 value used for fitting. We approximate the distribution of each spin coordinate as normal, with covariance given by the covariance of the true distribution. Based on equation 28, the covariance matrix is

$$\text{Cov}(\omega_i^*, \omega_j^*) = \frac{1}{4\omega^2} \left(1 - e^{-\sigma_\theta^2}\right) \left(1 - 3e^{-\sigma_\theta^2}\right) \begin{pmatrix} \omega_x^2 & \omega_x\omega_y & \omega_x\omega_z \\ \omega_x\omega_y & \omega_y^2 & \omega_y\omega_z \\ \omega_x\omega_z & \omega_y\omega_z & \omega_z^2 \end{pmatrix} + \frac{1}{4} \left(1 - e^{-2\sigma_\theta^2}\right) \mathbb{1}. \quad (29)$$

We then define the χ^2 statistic to be

$$\chi^2 = \sum_{i=0} (\boldsymbol{\omega}_i^* - \boldsymbol{\omega}_i)^T \text{Cov}^{-1}(\boldsymbol{\omega}_i^*, \boldsymbol{\omega}_j^*) (\boldsymbol{\omega}_i^* - \boldsymbol{\omega}_i) \quad (30)$$

where $\boldsymbol{\omega}_i$ is the i th expected spin and $\boldsymbol{\omega}_i^*$ is the data.

4 Results

5 Uncertainty Testing

6 Conclusion

References

- [1] Martin van Gelderen. The shift operators and translations of spherical harmonics. 1998.
- [2] Daniel Foreman-Mackey, David W. Hogg, Dustin Lang, and Jonathan B. Goodman. emcee: The mcmc hammer. *Publications of the Astronomical Society of the Pacific*, 125:306–312, 2013.